

# Theoretical and Computational Chemistry

Markus Meuwly\*

**Abstract:** Computer-based and theoretical approaches to chemical problems can provide atomistic understanding of complex processes at the molecular level. Examples ranging from rates of ligand-binding reactions in proteins to structural and energetic investigations of diastereomers relevant to organo-catalysis are discussed in the following. They highlight the range of application of theoretical and computational methods to current questions in chemical research.

**Keywords:** Globins · Molecular dynamics simulations · Organometallics · Proton transfer · Chemical reactions

## Markus Meuwly



Theoretical and Computational Chemistry at the Chemistry Department includes both the development of computational and theoretical concepts and their application to questions relevant

to chemistry and biophysics. One of the primary goals of the group of **Markus Meuwly** is to develop numerical methods and computational strategies to understand the energetics and dynamics of chemical reactions in complex environments and to apply them to chemically and biologically relevant systems.<sup>[1–7]</sup> Other activities concern the development of rapid methods for *in silico* screening of organometallic compounds,<sup>[8]</sup> the characterization of small-molecule dynamics in chromatographic systems,<sup>[9–11]</sup> and quantum nuclear effects in clusters and molecules.<sup>[12,13]</sup> In the following, representative applications together with the methods developed for their treatment are discussed.

## Rebinding Reactions in Proteins

Truncated hemoglobin N (trHbN) is a recently discovered heme protein found in plants, bacteria, and lower eukaryots. The trHbN of *Mycobacterium tuberculosis* has been proposed to play an important role in the survival of bacteria causing tuberculosis in host cells by converting toxic NO to harmless  $\text{NO}_3^-$ . Although the vertebrate Hb can perform the same reaction, the trHbN does it at least 20 times faster, with a second order rate constant of  $7.5 \times 10^8 \text{ M}^{-1}\text{s}^{-1}$ .<sup>[14]</sup> The fast reaction has been attributed to the presence of a continuous tunnel inside the protein matrix assisting ligand migration and due to the presence of ligand stabilizing residues in the active site of the protein (see Fig. 1).<sup>[14,15]</sup> However, an atomistic understanding of the detoxification reaction had remained elusive.

The following elementary four steps have been suggested to be involved in the overall detoxification reaction:<sup>[16]</sup>

- i)  $\text{Fe(II)} - \text{O}_2 + \text{NO} \rightarrow \text{Fe(III)} [-\text{OONO}]$
- ii)  $\text{Fe(III)} [-\text{OONO}] \rightarrow \text{Fe(IV)} = \text{O} + \text{NO}_2$
- iii)  $\text{Fe(IV)} = \text{O} + \text{NO}_2 \rightarrow \text{Fe(III)} [-\text{ONO}_2]$
- iv)  $\text{Fe(III)} [-\text{ONO}_2] \rightarrow \text{Fe(III)} + [\text{NO}_3]^-$

In the first step oxy-trHbN reacts with free NO and forms a peroxynitrite intermediate complex which then undergoes homolytic fission followed by the rebinding of free  $\text{NO}_2$  to the oxo-ferryl species to form the heme-bound nitrate complex which then undergoes heme-ligand dissociation resulting in free  $\text{NO}_3^-$  and pentacoordinated heme.

Computationally, each of the above processes is a reaction involving two states, each of which can be represented by a (usually high-dimensional) potential energy surface (PES). Reactions involving two PESs where quantum effects such as tunneling and coherence are less important can be effectively studied by force-field based classical molecular dynamics (MD)

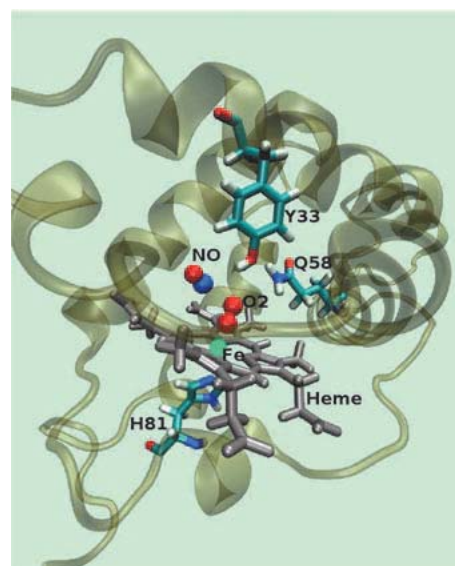


Fig. 1. Active site of truncated hemoglobin N with heme and a few important residues in explicit representation. The bound  $\text{O}_2$  and free NO ligands are shown in ball-and-stick representation.

simulations. Alternative approaches include mixed QM/MM methods, surface hopping or empirical valence bond theory.<sup>[17–19]</sup> The functional form of conventional force fields does not allow chemical bonds to be broken or formed and is therefore unsuitable to describe reactive processes. To overcome this limitation, together with his group, M. Meuwly developed a conceptually simple surface crossing approach to study reactive processes involving bond-formation and bond-breaking, suitable for high-dimensional systems within classical MD simulations.<sup>[20–23]</sup> The algorithm – adiabatic reactive molecular dynamics (ARMD) – is implemented in CHARMM.<sup>[24]</sup>

ARMD involves two potential energy surfaces defined by two sets of force field parameters corresponding to reactant ( $V_R$ ) and product ( $V_P$ ), differing by a limited number of force field parameters. The dynamics of the system is initiated and propa-

\*Correspondence: Prof. Dr. M. Meuwly  
Department of Chemistry  
University of Basel  
Klingelbergstrasse 80  
CH-4056 Basel  
Tel: +41 61 267 3821  
E-mail: m.meuwly@unibas.ch

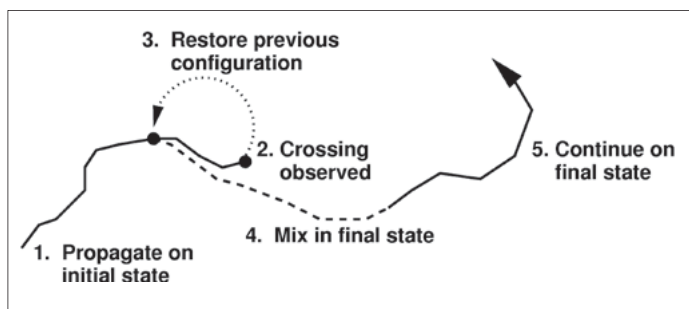


Fig. 2. Schematic of the adiabatic reactive MD method. The solid line represents propagation on the pure states and the dashed line corresponds to propagation on the mixed PES.

gated in the reactant state and the energy difference  $\Delta E = V_R - V_P + \Delta$  is monitored at each time step (Fig. 2). When  $\Delta E$  changes sign, a crossing is detected, the simulation is restored at a configuration prior to the crossing and the two potential energy surfaces are mixed over a finite time interval (typically several femtoseconds) to smoothly cross from product to educt. The force field parameters associated with the reactants and products of each of the reaction steps in the detoxification reaction are obtained from *ab initio* calculations or experimental data.

Each individual step (reactions i to iv) was then studied by running multiple ARMD trajectories.<sup>[23]</sup> For steps i, iii, and iv, the ARMD simulations yield rate constants on the picosecond time scale. However, for step ii of the detoxification reaction, ARMD simulations could not find crossings between the reactant and product despite running simulations of the order of nanoseconds.<sup>[23]</sup> From DFT calculations, it is known that this step involves a barrier of 6.7 kcal/mol.<sup>[25]</sup> Umbrella sampling simulations of step ii yield a barrier of 12–15 kcal/mol. A barrier of 6 to 12 kcal/mol corresponds to timescales on the order of micro- to milli-seconds. The ARMD simulations thus find that it is unlikely that the reaction proceeds *via* step ii but rather favour a reorganization reaction. This is in line with the lack of experimental detection of free  $\text{NO}_2$  in several studies which propose an alternative mechanism where the peroxyxynitrite intermediate rearranges to the nitrate complex.<sup>[26,27]</sup>

### Small Molecules as Spectroscopic Probes of Disordered Environments

Vibrational frequency shifts caused by external electric fields (Stark shifts), offer an increasingly important means to study the structure, electrostatics and dynamics of protein active sites.<sup>[28,29]</sup> The response of bond vibrational frequencies to changes in local electric fields can be accurately measured and used to probe heterogeneous chemical environments. However, while detailed spectroscopic data can be obtained it is usually difficult if not impossible to provide a structural interpretation

of the spectroscopic features. Force fields employed in many MD simulations allow extensive sampling, but are not sufficiently accurate to provide realistic response to local changes in electric field which is required for understanding vibrational spectroscopy.<sup>[30]</sup> Use of more detailed, multipolar charge models offers an attractive solution to more accurately describe the interaction of the probe molecule with the inhomogeneous electric fields in protein binding sites, while still allowing significant sampling of available phase space. In particular, it is possible to compare experimental and computed spectra and subsequently analyse the nuclear dynamics which provides a structural interpretation of the spectroscopic results. This has been successfully applied to the spectroscopy of CO in myoglobin, neuroglobin, and in ordered and disordered ices.<sup>[31]</sup>

### Proton Transfer in Malonaldehyde

From a computational point of view, hydrogen/proton transfer poses some unique challenges due to the intrinsic quantum nature of the H atom and due to the rapid motion of the proton. Ideally,

such processes are best studied employing quantum mechanics. In reality, such methods are computationally too demanding for routine applications. A popular alternative is to use QM/MM strategies where the reactive part is treated by quantum mechanics and the surrounding part by classical force fields. One variant of such a strategy has been developed by the Meuwly group which combines a quantum chemically determined potential energy surface, suitable for describing the proton transfer between a donor and an acceptor, with a force field to account for the remaining degrees of freedom.<sup>[32–34]</sup> Such an approach allows proton/hydrogen transfer to be followed with the speed of MD simulation and an accuracy comparable to QM/MM simulations. The total interaction energy for the system with coordinates  $\mathbf{Q}$  is given by

$$V(\mathbf{Q}) = V_{\text{PT}}(R, r, \theta) + V_{\text{MM}}(\mathbf{q}), \quad (1)$$

where the proton transfer motif, described by  $V_{\text{PT}}$ , is the QM determined potential energy surface along  $R$  (the distance between donor and acceptor atoms),  $r$  (the distance between donor and H atom), and  $\theta$  (the angle between the unit vectors along  $R$  and  $r$ ). The remaining degrees of freedom of the system ( $\mathbf{q}$ ) are described by a classical force field. The resulting potential is called Molecular Mechanics with Proton Transfer (MMPT).<sup>[32]</sup> In MD simulations with MMPT, the bonding pattern changes upon proton transfer. The algorithm is designed to add, modify, and remove force-field terms that include bonded and non-bonded interactions, in a smooth and energy conserving fashion.<sup>[32]</sup>

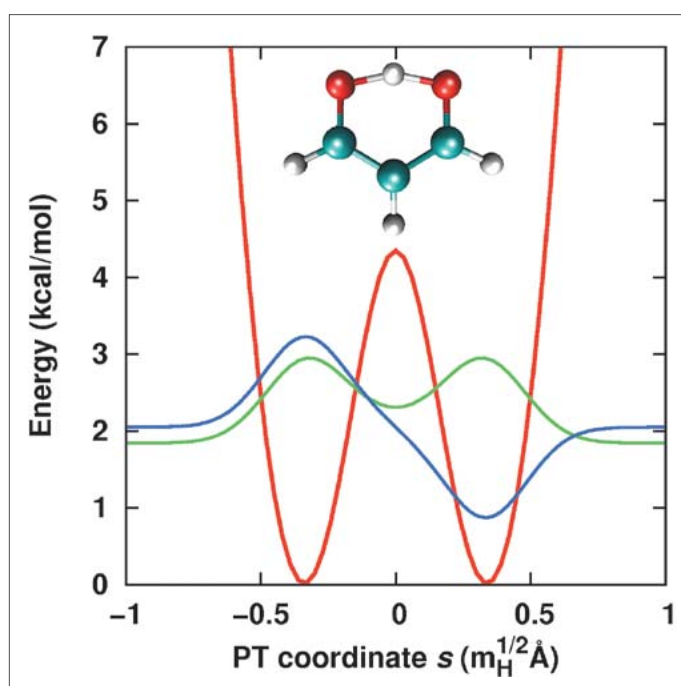


Fig. 3. Double well potential (red) for H-transfer in malonaldehyde. The transition state structure is given as ball-and-stick representation. The two lowest bound states with a splitting of  $22 \text{ cm}^{-1}$  are shown in green and blue, respectively.

Among various hydrogen bonded systems which are of current interest, malonaldehyde (MA, see Fig. 3) has been extensively studied. In particular, the infrared spectrum has been repeatedly recorded.<sup>[35–39]</sup> Nevertheless, the assignment of the H-transfer band is still not fully established and computational approaches employing accurate interaction potentials are required.<sup>[40]</sup> Furthermore, a large ground state splitting of 21.583 cm<sup>-1</sup> has been observed by different experiments with very high precision.<sup>[41,42]</sup> Such a splitting suggests rapid hydrogen transfer (with lifetimes of picoseconds). The ground state splitting can be computed from quantum calculations which are, however, impractical in full dimensionality. Therefore, a reduced Hamiltonian is developed based on the classical one-dimensional reaction path Hamiltonian,<sup>[43,44]</sup>

$$H(p_s, s, \{P_k, Q_k\}) = \sum_{k=1}^{3N-7} \left( \frac{1}{2} P_k^2 + \frac{1}{2} \omega_k^2(s) Q_k^2 \right) + V_0(s) + \frac{1}{2} \frac{[p_s - \sum_{k,l=1}^{3N-7} Q_k P_l B_{k,l}(s)]^2}{[1 + \sum_{k=1}^{3N-7} Q_k B_{k,3N-6}(s)]^2}, \quad (2)$$

where  $s$  is the hydrogen mass  $m_H$  weighted reaction coordinate and  $\{Q_k\}$  are the normal modes orthogonal to  $s$  with corresponding conjugate momenta  $\{P_k\}$ . Using a harmonic oscillator basis set for the ground state wavefunction of Eqn. (2) the reduced density can be derived by integrating out  $\{Q_k\}$ . Averaging Eqn. (2) over  $\{Q_k\}$  the one-dimensional harmonic bath approximated (HBA) Hamiltonian  $H^{\text{HBA}}$  is obtained:

$$H^{\text{HBA}}(p_s, s) \approx \frac{1}{2} \frac{p_s^2}{1 + \Delta_s} + V_0(s) + \sum_{k=1}^{3N-7} \frac{\omega_k(s)}{2} \left( 1 + \frac{\Delta_k}{1 + \Delta_s} \right), \quad (3)$$

which includes two non-negative contributions due to kinetic and potential couplings:  $\Delta_s(s) = \sum_k |\mathbf{B}_{k,3N-6}(s)|^2 / 2\omega_k(s)$  and  $\Delta_k(s) = \sum_l |\mathbf{B}_{l,k}(s)|^2 / 2\omega_l(s)$ . The term  $m^{\text{HBA}}(s) = 1 + \Delta_s$  plays the role of an effective mass which is larger than 1 (for H-transfer) due to kinetic couplings. Note that by working with  $H^{\text{HBA}}$  one is no longer treating the original H\* atom but a different ‘particle’ due to coupling to the bath modes  $\{Q_k\}$ . Fitting  $m^{\text{HBA}}$  to the observed splitting for H\*-tunneling (21.583 cm<sup>-1</sup>) and using mass-relationships be-

tween H\*- and D\*-transfer a calculated splitting for D\*-tunneling of 2.8 cm<sup>-1</sup> is obtained, which is in very good agreement with experiment (2.915 cm<sup>-1</sup>).<sup>[41,42,45]</sup> This also allows the vibrational fundamental for H\*-transfer to be located at 1573 cm<sup>-1</sup> which is supported by the finding of a low frequency O–H\* stretch mode (1672 cm<sup>-1</sup>) from a full dimensional RSH.<sup>[40]</sup>

### Capturing Electronic Effects with Force Fields

Determining low-energy structures of metal-containing catalysts is an important application for quantum chemical calculations. However, if the interaction between such a catalyst and the surrounding solvent is of explicit interest, or if chemical changes in the catalyst have to be screened for improved stability or chemical reactivity even the speed of state-of-the-art density functional theory (DFT) methods is not sufficient to allow meaningful characterization of the systems. It would be highly desirable to have suitable force fields for such purposes. VALBOND is a force field for organometallic compounds based on valence bond theory, where hybrid orbital strength functions are used for the molecular mechanics.<sup>[46–50]</sup> Following foundations laid by Pauling,<sup>[51,52]</sup> VALBOND aimed at correctly capturing bending potentials over a wide range of angular distortions which primarily determine the shape of molecules. VALBOND can describe both non-hypervalent and hypervalent molecules (not following the octet rule)<sup>[47]</sup> and transition metal complexes.<sup>[49,50]</sup> For hypervalent molecules, one has to take into account that there are several resonance structures, each described by a weighting factor  $c_j$ , which depends on the geometry. For a 3-center/4-electron bond (such as in ClF<sub>3</sub>) the total energy of the structure is the sum of three (formally equivalent) resonance structures each of which are mixed ionic-covalent Lewis structures. Assigning a bond order of 1 to one particular CF bond with the two other CF bonds having bond order 1/2 (and cyclic permutation) the total energy of CF<sub>3</sub> is given by  $E_{\text{tot}} = \sum_{j=1}^3 c_j E_j$  where  $c_j$  are mixing coefficients which depend on the molecular geometry. One choice for these mixing coefficients is<sup>[47]</sup>

$$c_j = \frac{\prod_{i=1}^{\text{hype}} \cos^2 \alpha_i}{\sum_{j=1}^{\text{config}} \prod_{i=1}^{\text{hype}} \cos^2 \alpha_i} \quad (4)$$

where the products run over all hypervalent angles  $i$  and *config* refers to the number of

resonance configurations. In general, the total energy is then given by

$$E_{\text{tot}} = \sum_j c_j E_j \quad (5)$$

where the sum is over all resonance configurations  $j$  with  $E_j$  the energy of a particular resonance configuration

$$E_j(\alpha) = \text{BOF} \times k_\alpha (1 - \Delta(\alpha + \pi)^2). \quad (6)$$

Here, BOF is the bond order factor,  $k_\alpha$  is a force constant,  $\Delta$  is the orbital overlap, and  $\alpha$  is the bond angle. The bond order factor (BOF) is the product of the formal bond orders of the two bonds described by the hybrid orbitals and standing at an angle  $\alpha$ .

To include explicit electronic effects, a generalized version – VAL-BONDTRANS – was developed in the Meuwly group.<sup>[8]</sup> The purpose of this additional development is to capture electronic effects related to the structural trans effect. Quadratic planar complexes, especially Pt(II) metal complexes, are known to exhibit a structural trans effect. In octahedral complexes trans effects can also occur, even if they are less pronounced.<sup>[53,54]</sup> One can distinguish between kinetic and a structural trans effect in an arrangement L1–M–L2. Here, L1 is trans to L2 which are both bonded to the metal M. The kinetic trans effect, originally discovered in the substitution rates of square planar Pt(II) complexes, depends on the specific reaction under consideration and its mechanism, and is not an explicit part of VAL-BONDTRANS. The structural or thermodynamic trans effect refers to the weakening of the M–L2 bond depending on the chemical identity of ligand L1. The structural effect may be seen in the bond lengthening of M–L2 or in the relative energies of different diastereomers. The performance of VAL-BONDTRANS with standard and fitted van der Waals parameters for an iridium(III)-PHOX catalyst is shown in Fig. 4.<sup>[8,55]</sup>

This last example highlights how force field development together with a combination of dedicated extensions can lead to computational strategies of potentially far-reaching implications for concrete chemical problems. With a rapid screening method that reproduces energies from quantum chemical calculations in the kcal/mol range it is possible to efficiently select the most promising low-energy diastereomers for a given organometallic catalyst. These pre-selected structures can be subjected to further refinement using more accurate methods. Furthermore, it is possible to include

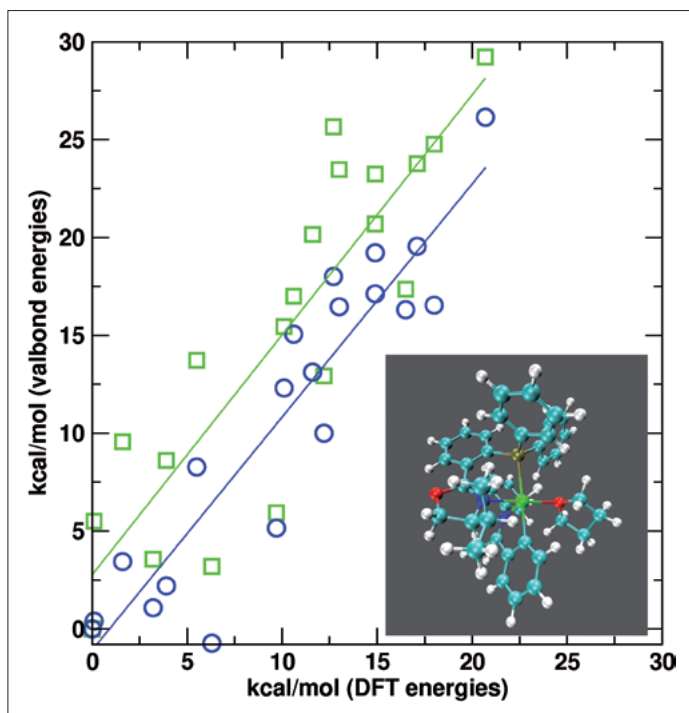


Fig. 4. Octahedral iridium(III)-PHOX catalyst with a triphenylphosphate coordinated group (inset) and performance of VAL-BONDTRANS in reproducing relative energetics from DFT calculations. Energies of all diastereomers of the Ir(III)-metal complex, using unoptimized Lennard-Jones parameters (green squares) and fitted Lennard-Jones parameters (blue circles). The fitting is carried out using the CHARMM/NoLLS interface.<sup>[55]</sup>

solvent effects beyond implicit models and to quantify entropic and enthalpic contributions. Finally, by combining several techniques, such as VAL-BONDTRANS and MMPT, it is even possible to study reactive processes involving organometallic compounds. Work along these lines is currently underway in collaboration with experimental groups.<sup>[56,57]</sup>

#### Acknowledgments

I thank all my coworkers, past and present, for their contribution to the work presented here and reflected in the citations. We are grateful for the financial support granted by the Schweizerischer Nationalfonds.

Received: October 15, 2010

- [1] D. R. Nutt, M. Meuwly, *Biophys. J.* **2003**, *85*, 3612.
- [2] D. R. Nutt, M. Meuwly, *Proc. Natl. Acad. Sci.* **2004**, *101*, 5998.
- [3] V. Zoete, M. Meuwly, *J. Chem. Phys.* **2004**, *121*, 4377.
- [4] M. Ladini, W. Leupin, M. Meuwly, M. Respondek, J. Wirz, V. Zoete, *Helv. Chim. Acta* **2005**, *88*, 53.
- [5] B. Christen, M. Christen, R. Paul, F. Schmid, M. Folcher, P. Jenoe, M. Meuwly, U. Jenal, *J. Biol. Chem.* **2006**, *281*, 32015.
- [6] F. F.-F. Schmid, M. Meuwly, *J. Mol. Biol.* **2007**, *374*, 1270.
- [7] S. Lammers, S. Lutz, M. Meuwly, *J. Comp. Chem.* **2008**, *29*, 1048.
- [8] I. Tubert-Brohman, M. Schmid, M. Meuwly, *J. Chem. Theo. Comp.* **2009**, *5*, 530.
- [9] A. Fouqueau, M. Meuwly, R. J. Bemish, *J. Phys. Chem. B* **2007**, *111*, 10208.
- [10] J. Braun, A. Fouqueau, R. J. Bemish, M. Meuwly, *PCCP* **2008**, *10*, 4765.
- [11] M. Orzechowski, M. Meuwly, *J. Phys. Chem. B* **2010**, *114*, 12203.
- [12] M. Meuwly, J. D. Doll, *J. Chem. Phys.* **2010**, *132*, 234315.

- [13] Y. Yang, M. Meuwly, *J. Chem. Phys.* **2010**, *133*, 064503.
- [14] H. Ouellet, Y. Ouellet, C. Richard, M. Labarre, B. Wittenberg, J. Wittenberg, M. Guertin, *Proc. Natl. Acad. Sci.* **2002**, *99*, 5902.
- [15] M. Milani, A. Pesce, Y. Ouellet, S. Dewilde, J. Friedmann, P. Ascenzi, M. Guertin, M. Bolognesi, *J. Biol. Chem.* **2004**, *279*, 21520.
- [16] J. L. Bourassa, E. L. Ives, A. L. Marqueling, R. Shimanovich, J. T. Groves, *J. Am. Chem. Soc.* **2001**, *123*, 5142.
- [17] P. A. Bash, M. J. Field, M. Karplus, *J. Am. Chem. Soc.* **1987**, *109*, 8092.
- [18] J. C. Tully, R. K. Preston, *J. Chem. Phys.* **1971**, *55*, 562.
- [19] A. Warshel, R. M. Weiss, *J. Am. Chem. Soc.* **1980**, *102*, 6218.
- [20] M. Meuwly, O. M. Becker, R. Stote, M. Karplus, *Biophys. Chem.* **2002**, *98*, 183.
- [21] D. R. Nutt, M. Meuwly, *Biophys. J.* **2006**, *90*, 1191.
- [22] J. Danielsson, M. Meuwly, *J. Chem. Theo. Comp.* **2008**, *4*, 1083.
- [23] S. Mishra, M. Meuwly, *J. Am. Chem. Soc.* **2010**, *132*, 2968.
- [24] B. R. Brooks, R. E. Bruccoleri, B. D. Olafson, D. J. States, S. Swaminathan, M. Karplus, *J. Comput. Chem.* **1983**, *4*, 18.
- [25] L. M. Blomberg, M. R. A. Blomberg, P. E. M. Siegbahn, *J. Biol. Inorg. Chem.* **2004**, *9*, 923.
- [26] S. Herold, M. Exner, T. Nausner, *Biochem.* **2001**, *40*, 3385.
- [27] S. Herold, *FEBS Letters* **1999**, *443*, 81.
- [28] S. G. Boxer, *J. Phys. Chem. B* **2009**, *113*, 2972.
- [29] L. J. Webb, S. G. Boxer, *Biochemistry* **2008**, *47*, 1588.
- [30] N. Plattner, M. Meuwly, *Biophys. J.* **2008**, *94*, 2505.
- [31] N. Plattner, M. Meuwly, *Chem. Phys. Chem.* **2008**, *9*, 1271.
- [32] S. Lammers, S. Lutz, M. Meuwly, *J. Comput. Chem.* **2008**, *29*, 1048.
- [33] S. Lammers, 'Simulations of proton transfer processes using reactive force fields', PhD thesis, University of Basel, **2006**.
- [34] S. Lammers, M. Meuwly, *Aust. J. Chem.* **2004**, *57*, 1223.
- [35] C. J. Seliskar, R. E. Hoffmann, *J. Mol. Spectrosc.* **1982**, *96*, 146.

- [36] Z. Smith, E. B. Wilson, *Spectrochim. Acta A* **1983**, *39*, 1117.
- [37] D. W. Firth, P. F. Barbara, H. P. Trommsdorff, *Chem. Phys.* **1989**, *136*, 349.
- [38] T. Chiavassa, R. Roubin, L. Piazzala, P. Verlaque, A. Allouche, F. Marinelli, *J. Phys. Chem.* **1992**, *96*, 10659.
- [39] C. Duan, D. Luckhaus, *Chem. Phys. Lett.* **2004**, *391*, 129.
- [40] D. P. Tew, N. C. Handy, S. Carter, *J. Chem. Phys.* **2006**, *125*, 084313.
- [41] S. L. Bauchcum, R. W. Duerst, W. F. Rowe, Z. Smith, E. B. Wilson, *J. Am. Chem. Soc.* **1981**, *103*, 6296.
- [42] D. W. Firth, K. Beyer, M. A. Dvorak, S. W. Reeve, A. Grushow, K. R. Leopold, *J. Chem. Phys.* **1991**, *94*, 1812.
- [43] W. H. Miller, N. C. Handy, J. E. Adams, *J. Chem. Phys.* **1979**, *72*, 99.
- [44] T. Carrington, W. H. Miller, *J. Chem. Phys.* **1984**, *81*, 3942.
- [45] S. L. Bauchcum, Z. Smith, E. B. Wilson, R. W. Duerst, *J. Am. Chem. Soc.* **1984**, *106*, 2260.
- [46] D. M. Root, C. R. Landis, T. Cleveland, *J. Am. Chem. Soc.* **1993**, *115*, 4201.
- [47] T. Cleveland, C. G. Landis, *J. Am. Chem. Soc.* **1996**, *118*, 6020.
- [48] C. R. Landis, T. K. Firman, D. M. Root, T. Cleveland, *J. Am. Chem. Soc.* **1998**, *120*, 1842.
- [49] C. R. Landis, T. Cleveland, T. K. Firman, *J. Am. Chem. Soc.* **1998**, *120*, 2641.
- [50] T. K. Firman, C. R. Landis, *J. Am. Chem. Soc.* **2001**, *123*, 11728.
- [51] L. Pauling, *Proc. Natl. Acad. Sci.* **1928**, *14*, 359.
- [52] L. Pauling, *J. Am. Chem. Soc.* **1931**, *53*, 1367.
- [53] J. V. Quagliano, L. Schubert, *Chem. Rev.* **1952**, *203*, 201.
- [54] B. J. Coe, S. J. Glenwright, *Coord. Chem. Rev.* **2000**, *203*, 5.
- [55] M. Devereux, M. Meuwly, *J. Chem. Inf. Model.* **2010**, *50*, 349.
- [56] U. Gellrich, W. Seiche, B. Breit, J. Huang, M. Meuwly, *J. Am. Chem. Soc.* **2010**, submitted.
- [57] J. Huang, U. Gellrich, W. Seiche, B. Breit, M. Meuwly, **2010**, in preparation.